

## Role of Layering Oscillations at Liquid Metal Surfaces in Bulk Recrystallization and Surface Melting

Orio Tomagnini,<sup>1</sup> Furio Ercolessi,<sup>2,3</sup> Simonetta Iarlori,<sup>1</sup> Francesco D. Di Tolla,<sup>2,3</sup> and Erio Tosatti<sup>2,3,4</sup>

<sup>1</sup>IBM-ECSEC, Viale Oceano Pacifico 171/173, I-00144 Rome, Italy

<sup>2</sup>Istituto Nazionale di Fisica della Materia (INFN), Italy

<sup>3</sup>International School for Advanced Studies (SISSA-ISAS), Via Beirut 4, I-34014 Trieste, Italy

<sup>4</sup>International Center For Theoretical Physics (ICTP), Trieste, Italy

(Received 1 August 1995)

The contrasting melting behavior of different surface orientations in metals can be explained in terms of a repulsive or attractive effective interaction between the solid-liquid and the liquid-vapor interfaces. We show how a crucial part of this interaction originates from the layering effects near the liquid metal surface. Its sign depends on the relative tuning of layering oscillations to the crystal interplanar spacing, thus explaining the orientational dependence. Molecular dynamics recrystallization simulations of Au surfaces provide direct and quantitative evidence of this phenomenon.

PACS numbers: 68.35.Rh, 68.35.Md, 68.45.Gd, 82.65.Dp

Surface melting (SM), i.e., complete wetting of a crystal surface by a thin film of its own melt, is very common in nature. For example, all faces of a real system, like rare gas solid Ar [1], as well as of its popular model, the fcc Lennard-Jones (LJ) crystal [2], are believed to melt completely. On the other hand, most metals have at least one close-packed face which does not melt, and is crystalline right up to  $T_m$  [3]. This nonmelting (NM) behavior is often explained phenomenologically, in terms of a low solid-vapor (SV) surface free energy  $\gamma_{SV}$ , which in this case can be lower than the sum of solid-liquid (SL) plus liquid-vapor (LV) interface free energies  $\gamma_{SL} + \gamma_{LV}$ . Open faces, by contrast, tend to have a higher energy when solid and this favors SM, in agreement with observations. At a more microscopic level, Chernov and Mikheev [4] made the interesting additional remark that surface nonmelting could, in fact, be ascribed to large minima in a strong oscillatory *effective* interaction between the SL and the LV interface. This oscillatory interaction is caused by a layering effect: The solid (similarly to a hard wall) induces in the liquid film a layerlike density oscillation with periodicity  $2\pi/Q_0$  [ $Q_0$  is the wave vector where the liquid structure factor  $S(Q)$  has its strongest peak], which in turn generates the interaction. Binding of the two interfaces in the deepest oscillation at  $\ell = 0$  is then responsible for a minimum of  $\gamma_{SV}$  and leads to NM. Alternatively, if the oscillations are weak, they can be washed out by capillary waves, the two interfaces unbind and there will be SM.

The purpose of this Letter is to argue theoretically, and to demonstrate through detailed simulations, that in non-LJ systems, particularly *in metals*, there are in reality not one, but two distinct layering oscillations—one with periodicity  $2\pi/Q_0$ , tied to the LV interface, and one with the periodicity of the interlayer spacing  $a$ , tied to the SL interface—which overlap and interfere inside a liquid metal film. Tuning and detuning of the two oscillations depends

on orientation, and may dramatically change the strength of the interaction, thus affecting deeply the surface melting behavior. In particular, while as expected well-tuned layering effects disfavor surface melting (and can make the close-packed surface very resistant to overheating), *the same does not happen for large detuning*, where SM is favored.

We will proceed in three stages. First, we give a qualitative, analytical argument showing that layering effects are strongly dependent on the orientation. Second, we make this more concrete through a model 1D wetting calculation [5] adapted to our case. Lastly, we present detailed surface recrystallization molecular dynamics (MD) nonequilibrium simulations which illustrate realistically the effect of attractive layering forces for a fcc (111) NM face, in contrast with a fcc (110) SM face where repulsion dominates.

Consider a liquid film of thickness  $\ell$ , wetting its own solid. The effective SL-LV interface interaction free energy can be written as  $f(\ell) = f_{SR}(\ell) + f_L(\ell)$  where  $f_{SR}$  is a short-range effective interaction, accounting for the merging of the two interfaces at close contact, and  $f_L$  is a residual part due to layering effects, which can be characterized as follows. The underlying solid propagates into the liquid film a first density oscillation roughly of the form  $\delta\rho_{SL}(z) \approx k_S \exp[-(z - z_{SL})/\xi_S] \cos(2\pi z/a)$  which has the periodicity of the (face-dependent) interlayer spacing  $a$ , and decays *outwards* from the SL interface center  $z_{SL}$  into the liquid ( $z$  grows going from solid to liquid to vapor) within some characteristic length  $\xi_S$  [5]. The LV interface of a metal originates, however, a *second* density oscillation  $\delta\rho_{LV}(z) \approx k_V \exp[(z - z_{LV})/\xi_V] \cos[(z - z_{LV})Q_0]$  which propagates *inwards*, with the typical liquid periodicity,  $2\pi/Q_0$ , and with a decay length  $\xi_V$  related to the peak width  $\delta Q$  in the liquid structure factor  $S(Q)$ ,  $2\pi/\xi_V \sim \delta Q$  [6]. This second oscillation is not universally present: it is only expected for

a strongly relaxed and contracted surface, like that of a metal, which represents a heavy disturbance for the liquid below [7]. In this sense, the LV interface in a metal is similar to a hard wall. By contrast, at the more disordered LJ liquid surface this oscillation (still present in principle) is below 2% [8] and practically irrelevant at  $T_m$ . A quantitative picture obtained by simulation (Fig. 1, described later) shows that a large oscillation is present for Au and absent in LJ. When  $\ell = z_{LV} - z_{SL}$  decreases, the two density oscillations overlap, giving rise, within linear response, to

$$f_L(\ell) = \frac{1}{2} \int d^3r d^3r' C(\mathbf{r} - \mathbf{r}') \delta\rho_{SL}(\mathbf{r}) \delta\rho_{LV}(\mathbf{r}'), \quad (1)$$

where the integration should be restricted to the liquid region  $z_{SL} \leq z \leq z_{LV}$ , and  $C(\mathbf{r} - \mathbf{r}')$  is the liquid density response function. Taking as a simple approximation for large  $r$  the form  $C(r) = C_0 \exp(-r/\xi) \cos(Q_0 r)$ , the integral can be carried out explicitly. The (111) surface corresponds to  $Q_0 a = 2\pi$ , and the (110) surface to  $Q_0 a = 2\pi\sqrt{3}/8$ . In both cases  $f_L(\ell)$  is oscillatory, with a wavelength  $2\pi/Q_0$  controlled by  $C(r)$ , and the lower envelope of the minima indicates interface attraction. However, as a consequence of tuning (commensurability), we find that the attractive minima of (1) are about 1 order of

magnitude deeper in the (111) case. Since the final surface melting behavior is determined by  $f_{SR}(\ell) + f_L(\ell)$ , the competition between SM and NM reduces, in our picture, to a matter of (a) how large  $f_{SR}$  (generally repulsive) is; (b) how important the liquid surface oscillation  $\delta\rho_{LV}$  is; and (c) how bad, or good, is the relative tuning of the two periodicities  $2\pi/Q_0$  and  $a$ . The binding energy between the SL and LV interfaces is given by  $\Delta\gamma \equiv \gamma_{SL} + \gamma_{LV} - \gamma_{SV} = \int_0^\infty [f'_{SR}(\ell) + f'_L(\ell)] d\ell$ . The above result suggests that  $f_L$  contributes much more to  $\Delta\gamma$  in a well-tuned case. In a poorly packed, poorly tuned face, the short-range repulsion cannot easily be reversed. In this case, fluctuations are very effective in washing out the shallow layering minima [4], whence a negative overall  $\Delta\gamma$ , leading to SM. In contrast, the good tuning of a well-packed face can cause  $f_L$  to prevail and yield the final  $\Delta\gamma > 0$  typical of a NM surface.

We have tested this qualitative picture by a microscopic 1D model calculation. We extend the Tarazona-Vicente (TV) scheme [5]—which demonstrates layering of a fluid near a wall—to describe a fluid confined between a wall (the LV interface) and a density-wave solid with adjustable periodicity. A 1D lattice-gas fluid (occupation  $\rho_i = 0, 1$ , lattice spacing equal to 1) is described by a grand canonical free energy

$$\Omega\{\rho_i\} = F\{\rho_i\} + \sum_i (V_i - \mu)\rho_i. \quad (2)$$

We take

$$F\{\rho_i\} = k_B T [\rho_i \ln \rho_i + (1 - \rho_i) \ln(1 - \rho_i)] - \alpha \rho_i \rho_{i+n} \quad (3)$$

so as to describe a simple fluid. The first term in (3) is entropic, and the second is a gradient, representing short-range order in the fluid, with periodicity  $2\pi/Q_0 \approx n$ . The external potential  $V_i$  consists of a hard wall at  $i = 0$  and of a semi-infinite “crystal” of periodicity  $a = \lambda n$  located at some very large distance  $i = L$  away. The hard wall generates a density oscillation decaying into the liquid from the left with periodicity  $n$ . The crystalline perturbation generates a second oscillation decaying into the liquid from the right, with periodicity  $\lambda n$ , where  $\lambda$  is a detuning parameter mimicking the crystalline interplanar spacing of a general surface orientation. The values of all the  $\rho_i$ 's are determined so as to minimize  $\Omega$ . As the crystal is moved closer and closer to the wall by reducing  $L$ , the fluid in between is modulated with both periodicities, and so is the excess of surface free energy  $\gamma(L) = \Omega(L) + PL$ , where  $P = k_B T \ln(1 - \rho) + \alpha \rho^2$  is the lattice-gas pressure [5]. The resulting surface free energy difference  $\Delta\gamma(L) \equiv \gamma(L) - \gamma(\infty)$  in the case  $\alpha/k_B T = -4$  (as used by TV for a strongly structured fluid) is shown in Fig. 2, together with density profiles. When the two periodicities are in tune ( $a = 2\pi/Q_0$ ), there is a sequence of attractive minima as a function of the thickness  $L$  (upper panel). Trapping in the deepest of these minima will correspond to NM, as discussed. When

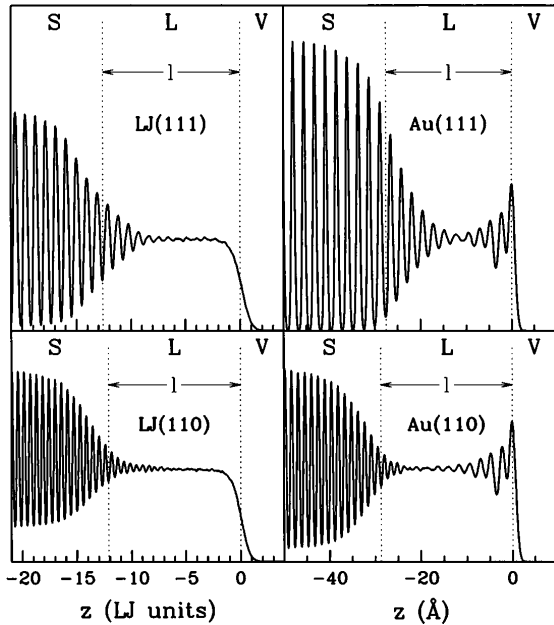


FIG. 1. Comparison between the ( $x, y$  averaged) density profiles of the (111) and (110) surfaces of LJ and Au, when wetted by a liquid film of thickness  $\ell \sim 30 \text{ \AA}$  (or  $\ell \sim 12$  LJ units), obtained by constant energy MD simulations. The film thickness is stabilized by energy conservation. Layering oscillations induced in the liquid film by the solid are present in all cases. The metal also exhibits a strong layering on the opposite side of the film, induced by the liquid surface. Its wavelength is rather different from that of the solid-induced oscillation in the case of Au(110), but very close for Au(111). Upon releasing the constant energy constraint at  $T \approx T_m$ , Au(111) is unstable and recrystallizes [9].

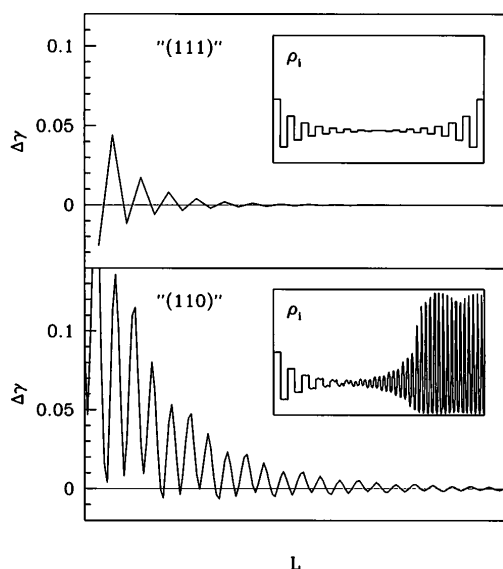


FIG. 2. Variation of the surface free energies  $\Delta\gamma$  (with respect to the infinite separation limit) as a function of the interface separation  $L$ , using the lattice-gas models described in the text. Upper panel: (111)-like case (in-tune perturbations). Lower panel: (110)-like case (out-of-tune perturbations). The lower envelope of the two curves shows strong interface attraction for “(111),” and weak attraction followed by repulsion at shorter distances for “(110).” Corresponding typical plots of densities  $\rho_i$  as a function of lattice site are shown in the insets. In the “(110)” case, the periodic potential induces crystal-like density oscillations for  $i > L$ .

tuning is absent (lower panel), the minima are still found, but there is no net attraction left. Prevalence of interface repulsion will favor SM in such a case.

The value of these concepts, if correct, should be readily recognizable in experiments (not yet available), or at least in a realistic MD simulation. For this purpose, we have conducted parallel simulations on Au(111) and Au(110), the former being a well-known NM face [10], and the latter a SM face [11]. We have used the “glue model” many-body potential [12], which reproduces correctly, among other things, the bulk melting temperature (within  $\sim 1\%$ ), the solid-vapor [12] and liquid-vapor [7] surface energies, the main surface reconstructions of gold [12], as well as the NM and SM behavior of these two surfaces [9,13,14]. MD simulations were done on a variety of systems, in the form of  $N$ -layer slabs ( $32 \leq N \leq 80$ ) with  $M$  atoms per layer ( $48 \leq M \leq 280$ ), one free surface and lateral periodic boundary conditions. Special care was taken in determining the effective bulk melting temperature, which in a cell-periodic system is both size and orientation dependent [14]. [For example, we find  $T_m = 1355 \pm 5$  K for a (111) bulk cell with  $N = 80$ ,  $M = 56$ , and  $T_m = 1327 \pm 3$  K for a (110) bulk cell with  $N = 32$ ,  $M = 280$ . These values are close to the actual  $T_m$  of Au, 1336 K.] Near  $T_m$ , we generate configurations [which can be of equilibrium on Au(110), and near equilibrium on Au(111)], where a certain number  $n$  of surface layers are melted. The density profiles of the two interfaces,

SL and LV, are shown in Fig. 1. The two oscillations, one attached to the LV interface, the other to the crystal, are clearly visible. As anticipated, their wavelengths are quite close for Au(111) ( $2\pi/Q_0 = 2.30 \pm 0.05$  Å,  $a = 2.39$  Å), and very different for Au(110) ( $a = 1.46$  Å).

In order to obtain information on the behavior of the total free energy as a function of  $\ell$ , we have developed a new method based on nonequilibrium recrystallization runs. Starting from a slab configuration with a large number of melted layers, the temperature  $T$  is suddenly reduced from an initial value  $T_i > T_m$  to a final value  $T < T_m$ . The SL interface moves towards its final equilibrium position with a velocity  $d\ell/dt$  (Fig. 3). As long as the liquid film is thick, the interface motion is approximately uniform. At small thickness, however, we find a final speedup for the (111) face but, in contrast, a final slowdown for the (110) face. The reverse experiment, i.e., fast melting, can also be done, and the reverse behavior is observed: initially, the melting front moves out quickly on (110), slowly on (111). By analyzing the behavior of  $\ell$  as a function of time  $t$ , we extract the effective SL-LV interaction free energy  $\bar{f}(\ell)$ , the average now fully including interface fluctuation effects. The driving force on the SL interface is given by  $-d\mathcal{F}/d\ell$ , where  $d\mathcal{F}$  is the change in the total free energy per unit area when the liquid thickness is changed from  $\ell$  to  $\ell + d\ell$ :

$$d\mathcal{F} = \rho L(1 - T/T_m)d\ell + \bar{f}(\ell + d\ell) - \bar{f}(\ell), \quad (4)$$

where  $\rho$  is the density of the liquid, and  $L$  the latent heat of melting. Close to  $T_m$ , the velocity may be assumed to be proportional to the driving force (classical body in a

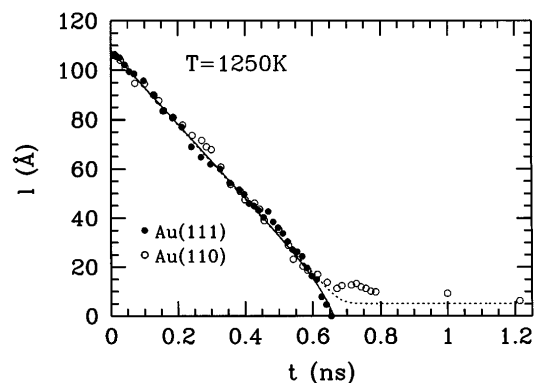


FIG. 3. Liquid thickness  $\ell$  as a function of time  $t$  as obtained from nonequilibrium MD quenching simulations from  $T = 1500$  K to  $T = 1250$  K  $\approx 0.93T_m$  for Au(111) (filled dots) and Au(110) (open dots). The starting point was in both cases a liquefied slab, more than 100 Å thick, sitting on top of a few (111) or (110) rigid crystalline layers. Curves corresponding to Eq. (6) are shown as a solid [(111)] and a dotted [(110)] line. Recrystallization proceeds at constant (but slightly orientation-dependent) speed until  $\ell \sim 40$  Å. For (111), the speed increases in the final stage [leading to a crystalline (111) surface], indicating attraction between the SL and the LV interface. The opposite occurs on (110), leading to a surface melted state. In this case the system reaches the equilibrium thickness near  $t \sim 1.2$  ns.

viscous medium):

$$\frac{d\ell}{dt} = -A[\rho L(1 - T/T_m) + \bar{f}'(\ell)]. \quad (5)$$

For  $\ell > 20 \text{ \AA}$ ,  $\bar{f}'(\ell)$  appears to be negligible, and we obtain  $A_{111} = 3.0 \times 10^{11} \text{ \AA}^4 \text{ s}^{-1} \text{ meV}^{-1}$  and  $A_{110} = 4.0 \times 10^{11} \text{ \AA}^4 \text{ s}^{-1} \text{ meV}^{-1}$ . We checked that they do not depend on  $T$  in the region of interest (within 100 K from  $T_m$ ). By assuming  $\bar{f}(\ell) = -\Delta\gamma \exp(-\ell/\xi)$ , Eq. (5) can be easily integrated, giving

$$\ell(t) = \xi \ln \left( C e^{-t/\tau} - \frac{\Delta\gamma}{\xi \rho L(1 - T/T_m)} \right), \quad (6)$$

where  $\tau = \xi/A\rho L(1 - T/T_m)$  and  $C$  is the integration constant, fixed by the initial liquid thickness  $\ell(0)$ . In the equilibrium limit  $t \rightarrow +\infty$ , and if  $\Delta\gamma < 0$ , Eq. (6) reduces to the well-known logarithmic growth law of  $\ell$  as a function of  $T$  [3]. From previous equilibrium or quasiequilibrium simulations [9,13,14] we extract (using also the relationship between maximum overheating temperature and  $\Delta\gamma$  [15])  $\Delta\gamma_{110} = -8.5 \pm 3.0 \text{ meV/\AA}^2$ ,  $\xi_{110} = 2.3 \pm 0.2 \text{ \AA}$ ,  $\Delta\gamma_{111} = +7.5 \pm 2.0 \text{ meV/\AA}^2$ ,  $\xi_{111} = 11 \pm 1 \text{ \AA}$ . Together with  $\rho = 0.0562 \text{ \AA}^{-3}$ ,  $L = 0.112 \text{ eV/atom}$  (known values for this potential) we calculate the theoretical  $\ell(t)$  from Eq. (6). This reproduces simulation data fairly well (Fig. 3), except where  $-d\mathcal{F}/d\ell$  becomes small and dynamics slows down [e.g.,  $\ell \lesssim 15 \text{ \AA}$  for (110)]. Clearly, the overall effective interaction free energy is *repulsive* in the (110) case, and *attractive* in the (111) case. Its magnitude is surprisingly large, as much as 10% of the total surface free energy ( $71 \text{ meV/\AA}^2$  for liquid Au at  $T_m$  [7]). The individual layering oscillations are generally not observable in the recrystallization interface velocity, washed out by the large intrinsic interface width, and by fluctuations. However, the large value of  $\xi_{111}$  shows that the (111) attraction is liquid mediated, and must therefore come from layering, as also suggested by Fig. 1. Conversely, the small value of  $\xi_{110}$  reflects the destructive interference of the two oscillations.

In summary, we have argued theoretically, and demonstrated both in a 1D model and realistic recrystallization simulations the changeable role of the layering on surface melting. The strong effect of the liquid sur-

face density oscillations, and their tuning-detuning effect has been demonstrated. Through x-ray detection of the magnitude of these oscillations, now possible [16], these results should shed new light on the high-temperature behavior of solid surfaces.

We acknowledge support from EEC under Contract No. ERBCHRXCT930342, and from CNR under Project SU-PALTEMP.

- 
- [1] J.G. Dash, *Contemp. Phys.* **30**, 89 (1989), and references therein.
  - [2] S. Valkealahti and R.M. Nieminen, *Phys. Scr.* **36**, 646 (1987); Y.J. Nikas and C. Ebner, *J. Phys. Condens. Matter* **1**, 2709 (1989); X.J. Chen *et al.*, *Surf. Sci.* **249**, 237 (1991); **264**, 207 (1992).
  - [3] J.F. van der Veen, B. Pluis, and A.W. Denier van der Gon, in *Chemistry and Physics of Solid Surfaces VII*, edited by R. Vanselow and R.F. Howe (Springer, Berlin, 1988), p. 455.
  - [4] A.A. Chernov and L.V. Mikheev, *Phys. Rev. Lett.* **60**, 2488 (1988); *Physica (Amsterdam)* **157A**, 1042 (1989).
  - [5] P. Tarazona and L. Vicente, *Mol. Phys.* **56**, 557 (1985).
  - [6] Such a component in  $\delta\rho_{SL}$ , hypothesized in Ref. [4], is in practice not found (see Fig. 1).
  - [7] S. Iarlori, P. Carnevali, F. Ercolessi, and E. Tosatti, *Surf. Sci.* **211/212**, 55 (1989).
  - [8] D.L. Heath and J.K. Percus, *J. Stat. Phys.* **49**, 319 (1987); M.J.P. Nijmeijer *et al.*, *J. Chem. Phys.* **89**, 3789 (1988).
  - [9] P. Carnevali, F. Ercolessi, and E. Tosatti, *Phys. Rev. B* **36**, 6701 (1987).
  - [10] K.D. Stock and B. Grosser, *J. Cryst. Growth* **50**, 485 (1980).
  - [11] A. Hoss, M. Nold, P. von Blanckenhagen, and O. Meyer, *Phys. Rev. B* **45**, 8714 (1992).
  - [12] F. Ercolessi, M. Parrinello, and E. Tosatti, *Philos. Mag. A* **58**, 213 (1988).
  - [13] F. Ercolessi, S. Iarlori, O. Tomagnini, E. Tosatti, and X.J. Chen, *Surf. Sci.* **251/252**, 645 (1991).
  - [14] F. Ercolessi, O. Tomagnini, S. Iarlori, and E. Tosatti, in *Nanosources and Manipulation of Atoms Under High Fields and Temperatures: Applications*, edited by Vu Thien Binh, N. Garcia, and K. Dransfeld (Kluwer, Dordrecht, 1993), p. 185.
  - [15] F.D. Di Tolla, F. Ercolessi, and E. Tosatti, *Phys. Rev. Lett.* **74**, 3201 (1995).
  - [16] O. Magnussen *et al.*, *Phys. Rev. Lett.* **74**, 4444 (1995).